Appl. Phys. A (2016) 122:843
DOI 10.1007/s00339-016-0368-1

Applied Physics A
Materials Science & Processing

Wave propagation analysis of quasi-3D FG nanobeams in thermal environment based on nonlocal strain gradient theory

Farzad Ebrahimi[1] · Mohammad Reza Barati[1]

Received: 13 May 2016 / Accepted: 12 August 2016 / Published online: 23 August 2016

Abstract This article examines the application of nonlocal strain gradient elasticity theory to wave dispersion behavior of a size-dependent functionally graded (FG) nanobeam in thermal environment. The theory contains two scale parameters corresponding to both nonlocal and strain gradient effects. A quasi-3D sinusoidal beam theory considering shear and normal deformations is employed to present the formulation. Mori–Tanaka micromechanical model is used to describe functionally graded material properties. Hamilton's principle is employed to obtain the governing equations of nanobeam accounting for thickness stretching effect. These equations are solved analytically to find the wave frequencies and phase velocities of the FG nanobeam. It is indicated that wave dispersion behavior of FG nanobeams is significantly affected by temperature rise, nonlocality, length scale parameter and material composition.

1 Introduction

Functionally graded materials (FGMs) have a continuous material variation in one or more dimensions, from one surface to another. Hence, these materials have the potential to remove the stress concentration observable in laminated composites. FGMs are generally isotropic and nonhomogeneous and are composed from a mixture of ceramics and metals to obtain a composition that possesses a favorable application, especially in thermal environments [1–4]. Therefore, it is important to discover mechanical specifications of these material structures. Hence, FGMs have received a wide attention from engineers and researchers because of notable applications in several fields including mechanical, civil and aerospace engineering. Therefore, it is important to study the wave propagation in structures made of FG materials. Chakraborty and Gopalakrishnan [5] researched axial–flexural–shear coupled wave propagation of lengthwise graded beams. Also, Chakraborty and Gopalakrishnan [6] studied wave propagation of FG beams by using spectrally formulated finite element. Wave dispersion and transient response of higher-order shear deformable FG plates investigated by Sun and Luo [7, 8]. Chen et al. [9] researched dispersion curves of waves in FG plates. Thermoelastic wave propagation of temperature-dependent FG plates investigated by Sun and Luo [7]. They assumed that the temperature field varies in the thickness direction only and has a uniform distribution over the plate surface. Finally, they explored that the frequency and phase velocity of the wave propagation decrease by increasing in the temperature. Wave propagation of porous FG plates employing various higher-order shear deformation theories is investigated by Yahia et al. [10]. They concluded that higher-order theories can accurately predict the wave characteristics of FG structures, and only a little difference exists between their results. Also, many paper are published concerning with analysis of FGM structures based on higher-order shear deformation theories [11–13].

Nanoscale structures are of significance in the field of nano-mechanics, so it is crucial to account for small size influences in their mechanical analysis. The lack of a scale parameter in the classical continuum theory makes it impossible to describe the size effects [1, 14]. Hence, size-

✉ Farzad Ebrahimi
febrahimy@eng.ikiu.ac.ir

[1] Department of Mechanical Engineering, Faculty of Engineering, Imam Khomeini International University, Qazvin, Iran

dependent continuum theories such as nonlocal elasticity theory [15, 16] are developed to consider the small-scale effects. Application of nonlocal elasticity theory to wave propagation of nanoscale structures is examined by several researchers. Investigation of wave dispersion behavior of double-walled carbon nanotubes using nonlocal Timoshenko beam model is carried out by Yang et al. [17]. Assadi and Farshi [18] conducted nonlocal axial and transverse wave propagation of nanotubes resting on elastic foundation considering surface effects. Wave propagation analysis of single-walled carbon nanotubes exposed to an axial magnetic field based on nonlocal Euler–Bernoulli beam model researched by Narendar et al. [19]. Arani et al. [20] performed wave propagation of bonded double-piezoelectric nanoscale beams. Recently, Eltaher et al. [21] presented a review on nonlocal elastic models for bending, buckling, vibrations and wave propagation of nanoscale beams.

Recently, with the development in nanotechnology, FGMs have also been employed in MEMS/NEMS. Actually, FGMs find increasing applications in micro- and nanoscale structures such as thin films in the form of shape memory alloys [22], atomic force microscopes (AFMs) [23], nano-sensors and nano-actuator. In all of these applications, the size effect plays major role which should be considered to study the mechanical behaviors of such small-scale structures. Hence, analysis of FG nanostructures have also been of interest of many investigators. Analysis of vibration behavior of FG nanobeams using finite element method is carried out by Eltaher et al. [24]. Vibrational behavior of nanoscale FGM beams under thermal loadings is studied by Ebrahimi and Salari [25]. Ebrahimi and Barati [26] presented Dynamic modeling of a thermo–piezo-electrically actuated nanosize FG beam subjected to a magnetic field. Also, Ebrahimi and Barati [27–30] presented vibration and buckling analysis of smart piezoelectrically actuated FG nanobeams subjected to various physical fields. In another paper, Ebrahimi and Barati [31] examined small-scale effects on hygro-thermo-mechanical vibration of temperature-dependent FG nanoscale beams. Recently, analysis of FG nanostructures using shear deformation theories has gained great attention by several researchers. Tounsi et al. [32] proposed a nonlocal refined beam theory for deflection, buckling and vibration of FGM beams. Bounouara et al. [33] presented a nonlocal zeroth-order shear deformation theory for free vibration of functionally graded nanoscale plates resting on elastic foundation. Belkorissat et al. [34] investigated vibration properties of functionally graded nanoplates using a new nonlocal refined four variable model. Most recently, Barati and Shahverdi [35] presented an analytical solution for thermal vibration of compositionally graded nanoplates with arbitrary boundary conditions based on physical neutral surface position. In these papers on shear deformation theories, thickness stretching effect is neglected. So, it is also possible to extend these theories accounting for thickness stretching effect [36–38].

Strain gradient elasticity theory reports a stiffness-hardening impact on the nanobeam structure which is neglected in nonlocal elasticity theory of Eringen [39]. Recently, Lim et al. [40] introduced the nonlocal strain gradient theory which contains two scale parameters into a single theory. The nonlocal strain gradient theory captures the true influence of the two length scale parameters on the physical and mechanical behavior of small size structures. Also, Li et al. [41] performed vibration analysis of nonlocal strain gradient FG nanobeams. They mentioned that the vibration frequencies can generally increase with the increasing in length scale parameter or the decreasing nonlocal parameter. Also, Li et al. [42] performed flexural wave propagation analysis of size-dependent FG beams based on nonlocal strain gradient theory. Ebrahimi and Barati [43] performed flexural wave propagation analysis of S-FGM Nanobeams under longitudinal magnetic field based on nonlocal strain gradient theory. Most recently, Ebrahimi et al. [44] presented a nonlocal strain gradient theory for wave propagation analysis in temperature-dependent inhomogeneous nanoplates. The literature survey reveals that wave dispersion analysis of quasi-3D FG nanobeams in thermal environment based on nonlocal strain gradient theory is an interesting topic which is not carried out till to now.

In this paper, a quasi-3D beam model is developed for wave propagation analysis of FG nanobeams in thermal environments based on nonlocal strain gradient theory in which the stress accounts not only for nonlocal elastic stress field but also for the strain gradients stress field. Material properties of the nanobeam change gradually based on Mori–Tanaka model. Applying an analytical solution, the dispersion, phase velocity and group velocity curves of the wave propagation of FG nanobeam under thermal loading are plotted and the characteristics of wave propagation of the FG nanobeam are explained in detail. Several examples are provided to show the importance of nonlocal parameter, length scale parameter, temperature rise and gradient index on wave propagation characteristics of FG nanobeams.

2 Theory and formulation

2.1 Mori–Tanaka FGM nanobeam model

Mori–Tanaka homogenization model represents the effective material properties including effective local bulk modulus K_e and shear modulus μ_e in the form [35]:

$$\frac{K_e - K_m}{K_c - K_m} = \frac{V_c}{1 + V_m (K_c - K_m)/(K_m + 4\mu_m/3)} \tag{1}$$

$$\frac{\mu_e - \mu_m}{\mu_c - \mu_m} = \frac{V_c}{1 + V_m(\mu_c - \mu_m)/[(\mu_m + \mu_m(9K_m + 8\mu_m)/(6(K_m + 2\mu_m))]} \tag{2}$$

where subscripts m and c denote metal and ceramic, respectively, and their volume fractions are related by:

$$V_c + V_m = 1 \tag{3}$$

The volume fraction of the ceramic phase is given by:

$$V_c = \left(\frac{z}{h} + \frac{1}{2}\right)^p \tag{4}$$

Here, p represents the gradient index which determines gradual variation of material properties through the thickness of the nanobeam. Finally, the effective Young's modulus (E), poison ratio (v) and mass density (ρ) can be expressed by:

$$E(z) = \frac{9K_e \mu_e}{3K_e + \mu_e} \tag{5}$$

$$v(z) = \frac{3K_e - 2\mu_e}{6K_e + 2\mu_e} \tag{6}$$

$$\rho(z) = \rho_c V_c + \rho_m V_m \tag{7}$$

The thermal expansion coefficient (α) and thermal conductivity (κ) may be expressed by

$$\frac{\alpha_e - \alpha_m}{\alpha_c - \alpha_m} = \frac{\frac{1}{K_e} - \frac{1}{K_m}}{\frac{1}{K_c} - \frac{1}{K_m}} \tag{8}$$

$$\frac{\kappa_e - \kappa_m}{\kappa_c - \kappa_m} = \frac{V_c}{1 + V_m \frac{(\kappa_c - \kappa_m)}{3\kappa_m}} \tag{9}$$

Also, temperature-dependent coefficients of material phases can be expressed according to the following relation:

$$P = P_0\left(P_{-1}\, T^{-1} + 1 + P_1\, T + P_2\, T^2 + P_3\, T^3\right) \tag{10}$$

where P_0, P_{-1}, P_1, P_2 and P_3 are the temperature-dependent constants which are tabulated in Table 1 for Si_3N_4 and SUS 304. The bottom and top surfaces of FG nanobeam are fully metal (SUS 304) and fully ceramic (Si_3N_4), respectively.

In this study, the temperature varies nonlinearly through the thickness. Temperature distribution can be obtained by solving the steady-state heat conduction equation with the boundary conditions on bottom- and top surfaces of the nanobeam across the thickness:

$$-\frac{d}{dz}\left(\kappa(z,\ T)\frac{dT}{dz}\right) = 0 \tag{11}$$

Considering the boundary conditions

$$T\left(\frac{h}{2}\right) = T_c, \quad T\left(-\frac{h}{2}\right) = T_m \tag{12}$$

The solution of above equation is:

$$T = T_m + (T_c - T_m)\frac{\int_{-\frac{h}{2}}^{z} \frac{1}{\kappa(z,T)} dz}{\int_{-\frac{h}{2}}^{\frac{h}{2}} \frac{1}{\kappa(z,T)} dz} \tag{13}$$

where $\Delta T = T_c - T_m$ is the temperature change.

2.2 Kinematic relations

The displacement field of FG nanobeam based on quasi-3D beam theory can be expressed by:

$$u_x(x,z) = u(x) - z\frac{\partial w_b}{\partial x} - f(z)\frac{\partial w_s}{\partial x} \tag{14}$$

$$u_z(x,z) = w_b(x) + w_s(x) + g(z)w_z(x) \tag{15}$$

where u is longitudinal displacement and w_b, w_s denote the components correspond to the bending and shear transverse displacements of a point on the beam mid-surface, respectively. Also, $f(z)$ is the shape function representing the shear stress/strain distribution through the beam thickness. The present theory has a trigonometric function in the form:

$$f(z) = z - \sin(\xi z)/\xi \tag{16}$$

where $\xi = \pi/h$. Nonzero strains of the present beam model can be expressed as follows:

$$\varepsilon_{xx} = \frac{\partial u}{\partial x} - z\frac{\partial^2 w_b}{\partial x^2} - f(z)\frac{\partial^2 w_s}{\partial x^2}, \quad \varepsilon_{zz} = \frac{\partial g(z)}{\partial z}\frac{\partial w_z}{\partial x} \tag{17}$$

$$\gamma_{xz} = g\left(\frac{\partial w_s}{\partial x} + \frac{\partial w_z}{\partial x}\right) \tag{18}$$

where $g(z) = 1 - df/dz$. Also, the Hamilton's principle states that:

$$\int_0^t \delta(U + V - K)\, dt = 0 \tag{19}$$

Here, U is strain energy, V is work done by external forces, and K is kinetic energy. The virtual strain energy can be written as:

$$\delta U = \int_v \sigma_{ij}\delta\, \varepsilon_{ij}\, dV = \int_v (\sigma_{xx}\delta\, \varepsilon_{xx} + \sigma_{xz}\delta\, \gamma_{xz})\, dV \tag{20}$$

Substituting Eqs. (17) and (18) into Eq. (20) yields:

$$\delta U = \int_0^L \left(N\frac{d\delta u}{dx} - M_b\frac{d^2\delta w_b}{dx^2} - M_s\frac{d^2\delta w_s}{dx^2} + Q\left(\frac{d\delta w_s}{dx} + \frac{d\delta w_z}{dx}\right) + R_z\delta w_z\right)dx \tag{21}$$

Table 1 Temperature-dependent coefficients for Si_3N_4 and SUS 304

Material	Properties	P_0	P_{-1}	P_1	P_2	P_3
Si_3N_4	E (Pa)	348.43e+9	0	−3.070e−4	2.160e−7	−8.946e−11
	α (K^{-1})	5.8723e−6	0	9.095e−4	0	0
	ρ (Kg/m^3)	2370	0	0	0	0
	κ (W/mK)	13.723	0	−1.032e−3	5.466e−7	−7.876e−11
	ν	0.24	0	0	0	0
SUS 304	E (Pa)	201.04e+9	0	3.079e−4	−6.534e−7	0
	α (K^{-1})	12.330e−6	0	8.086e−4	0	0
	ρ (Kg/m^3)	8166	0	0	0	0
	κ (W/mK)	15.379	0	−1.264e−3	2.092e−6	−7.223e−10
	ν	0.3262	0	−2.002e−4	3.797e−7	0

in which the variables expressed in the above equation are defined as follows:

$$N=\int_A \sigma_{xx}\,\mathrm{d}A,\quad M_\mathrm{b}=\int_A z\sigma_{xx}\mathrm{d}A,\quad M_\mathrm{s}=\int_A f\sigma_{xx}\mathrm{d}A,$$
$$Q=\int_A g\sigma_{xz}\,\mathrm{d}A,\quad R_z=\int_A g'\sigma_{zz}\,\mathrm{d}A \tag{22}$$

The first variation of the work done by applied forces can be written in the form:

$$\delta V=\int_0^L\left(N_1^T\left(\frac{d(w_\mathrm{b}+w_\mathrm{s})}{\mathrm{d}x}\frac{d\delta(w_\mathrm{b}+w_\mathrm{s})}{\mathrm{d}x}\right)+N_2^T\left(\frac{\mathrm{d}w_z}{\mathrm{d}x}\frac{\mathrm{d}\delta w_z}{\mathrm{d}x}\right)\right)\mathrm{d}x \tag{23}$$

where N_1^T and N_2^T are applied force due to temperature change as:

$$N_1^T=\int_{-h/2}^{h/2}E(z,T)\,\alpha(z,T)\,(T-T_0)\,\mathrm{d}z,$$
$$N_2^T=\int_{-h/2}^{h/2}g(z)E(z,T)\,\alpha(z,T)\,(T-T_0)\,\mathrm{d}z \tag{24}$$

where T_0 is the reference temperature. The variation of kinetic energy is presented by:

$$\begin{aligned}\delta K=\int_0^L\Bigg(&I_0\left[\frac{\mathrm{d}u}{\mathrm{d}t}\frac{\mathrm{d}\delta u}{\mathrm{d}t}+\left(\frac{\mathrm{d}w_\mathrm{b}}{\mathrm{d}t}+\frac{\mathrm{d}w_\mathrm{s}}{\mathrm{d}t}\right)\left(\frac{\mathrm{d}\delta w_\mathrm{b}}{\mathrm{d}t}+\frac{\mathrm{d}\delta w_\mathrm{s}}{\mathrm{d}t}\right)\right]\\
&-I_1\left(\frac{\mathrm{d}u}{\mathrm{d}t}\frac{\mathrm{d}^2\delta w_\mathrm{b}}{\mathrm{d}x\mathrm{d}t}+\frac{\mathrm{d}^2w_\mathrm{b}}{\mathrm{d}x\mathrm{d}t}\frac{\mathrm{d}\delta u}{\mathrm{d}t}\right)+I_2\left(\frac{\mathrm{d}^2w_\mathrm{b}}{\mathrm{d}x\mathrm{d}t}\frac{\mathrm{d}^2\delta w_\mathrm{b}}{\mathrm{d}x\mathrm{d}t}\right)\\
&-J_1\left(\frac{\mathrm{d}u}{\mathrm{d}t}\frac{\mathrm{d}^2\delta w_\mathrm{s}}{\mathrm{d}x\mathrm{d}t}+\frac{\mathrm{d}^2w_\mathrm{s}}{\mathrm{d}x\mathrm{d}t}\frac{\mathrm{d}\delta u}{\mathrm{d}t}\right)+K_2\left(\frac{\mathrm{d}^2w_\mathrm{s}}{\mathrm{d}x\mathrm{d}t}\frac{\mathrm{d}^2\delta w_\mathrm{s}}{\mathrm{d}x\mathrm{d}t}\right)\\
&+J_2\left(\frac{\mathrm{d}^2w_\mathrm{b}}{\mathrm{d}x\mathrm{d}t}\frac{\mathrm{d}^2\delta w_\mathrm{s}}{\mathrm{d}x\mathrm{d}t}+\frac{\mathrm{d}^2w_\mathrm{s}}{\mathrm{d}x\mathrm{d}t}\frac{\mathrm{d}^2\delta w_\mathrm{b}}{\mathrm{d}x\mathrm{d}t}\right)\\
&+I_\mathrm{g}\left(\frac{\mathrm{d}^2(w_\mathrm{b}+w_\mathrm{s})}{\mathrm{d}x\mathrm{d}t}\frac{\mathrm{d}^2\delta w_z}{\mathrm{d}x\mathrm{d}t}+\frac{\mathrm{d}^2w_z}{\mathrm{d}x\mathrm{d}t}\frac{\mathrm{d}^2\delta(w_\mathrm{b}+w_\mathrm{s})}{\mathrm{d}x\mathrm{d}t}\right)\\
&+K_\mathrm{g}\left(\frac{\mathrm{d}^2w_z}{\mathrm{d}x\mathrm{d}t}\frac{\mathrm{d}^2\delta w_z}{\mathrm{d}x\mathrm{d}t}\right)\Bigg)\mathrm{d}x\end{aligned} \tag{25}$$

where

$$(I_0,I_1,J_1,I_2,J_2,K_2)=\int_{-h/2}^{h/2}\rho(z)(1,z,f,z^2,zf,f^2)\mathrm{d}z$$
$$(I_\mathrm{g},K_\mathrm{g})=\int_{-h/2}^{h/2}\rho(z)(g,g^2)\mathrm{d}z \tag{26}$$

The following equations are obtained by inserting Eqs. (21)–(25) in Eq. (19) when the coefficients of δu, δw_b, δw_s and δw_z are equal to zero:

$$\frac{\partial N}{\partial x}=I_0\frac{\mathrm{d}^2u}{\mathrm{d}t^2}-I_1\frac{\mathrm{d}^3w_\mathrm{b}}{\mathrm{d}x\mathrm{d}t^2}-J_1\frac{\mathrm{d}^3w_\mathrm{s}}{\mathrm{d}x\mathrm{d}t^2} \tag{27}$$

$$\begin{aligned}&\frac{\mathrm{d}^2M_\mathrm{b}}{\mathrm{d}x^2}-N_1^T\frac{\mathrm{d}^2(w_\mathrm{b}+w_\mathrm{s})}{\mathrm{d}x^2}-N_2^T\frac{\mathrm{d}^2w_z}{\mathrm{d}x^2}=+I_0\left(\frac{\mathrm{d}^2w_\mathrm{b}}{\mathrm{d}t^2}+\frac{\mathrm{d}^2w_\mathrm{s}}{\mathrm{d}t^2}\right)\\
&\quad+I_1\frac{\mathrm{d}^3u}{\mathrm{d}x\mathrm{d}t^2}-I_2\frac{\mathrm{d}^4w_\mathrm{b}}{\mathrm{d}x^2\mathrm{d}t^2}-J_2\frac{\mathrm{d}^4w_\mathrm{s}}{\mathrm{d}x^2\mathrm{d}t^2}+I_\mathrm{g}\frac{\mathrm{d}^2w_z}{\mathrm{d}t^2}\end{aligned} \tag{28}$$

$$\begin{aligned}&\frac{\mathrm{d}^2M_\mathrm{s}}{\mathrm{d}x^2}+\frac{\mathrm{d}Q}{\mathrm{d}x}-N_1^T\frac{\mathrm{d}^2(w_\mathrm{b}+w_\mathrm{s})}{\mathrm{d}x^2}-N_2^T\frac{\mathrm{d}^2w_z}{\mathrm{d}x^2}\\
&\quad=+I_0\left(\frac{\mathrm{d}^2w_\mathrm{b}}{\mathrm{d}t^2}+\frac{\mathrm{d}^2w_\mathrm{s}}{\mathrm{d}t^2}\right)+J_1\frac{\mathrm{d}^3u}{\mathrm{d}x\mathrm{d}t^2}-J_2\frac{\mathrm{d}^4w_\mathrm{b}}{\mathrm{d}x^2\mathrm{d}t^2}\\
&\qquad-K_2\frac{\mathrm{d}^4w_\mathrm{s}}{\mathrm{d}x^2\mathrm{d}t^2}+I_\mathrm{g}\frac{\mathrm{d}^2w_z}{\mathrm{d}t^2}\end{aligned} \tag{29}$$

$$\begin{aligned}&\frac{\mathrm{d}Q}{\mathrm{d}x}-R_z-N_1^T\frac{\mathrm{d}^2(w_\mathrm{b}+w_\mathrm{s})}{\mathrm{d}x^2}-N_2^T\frac{\mathrm{d}^2w_z}{\mathrm{d}x^2}\\
&\quad=+I_g\left(\frac{\mathrm{d}^2w_\mathrm{b}}{\mathrm{d}t^2}+\frac{\mathrm{d}^2w_\mathrm{s}}{\mathrm{d}t^2}\right)+K_\mathrm{g}\frac{\mathrm{d}^2w_z}{\mathrm{d}t^2}.\end{aligned} \tag{30}$$

2.3 The nonlocal FG nanobeam strain gradient model

Nonlocal strain gradient elasticity [44] enumerates the stress for both nonlocal stress and strain fields. Therefore, the stress can be expressed by:

$$\sigma_{ij} = \sigma_{ij}^{(0)} - \frac{d\sigma_{ij}^{(1)}}{dx} \tag{31}$$

where the stresses $\sigma_{xx}^{(0)}$ and $\sigma_{xx}^{(1)}$ are related to strain ε_{xx} and strain gradient $\varepsilon_{xx,x}$, respectively, and are defined as:

$$\sigma_{ij}^{(0)} = \int_0^L C_{ijkl}\alpha_0(x,x',e_0a)\varepsilon'_{kl}(x')dx' \tag{32a}$$

$$\sigma_{ij}^{(1)} = l^2\int_0^L C_{ijkl}\alpha_1(x,x',e_1a)\varepsilon'_{kl,x}(x')dx' \tag{32b}$$

in which C_{ijkl} are the elastic constants and e_0a and e_1a take into account the effect of nonlocal stress field, and l is the length scale parameter and introduces the influence of higher-order strain gradient stress field. When the nonlocal functions $\alpha_0(x, x', e_0a)$ and $\alpha_1(x, x', e_1a)$ satisfy the developed conditions by Eringen [16], the constitutive relation for a FGM nanobeam can be stated as:

$$\left[1-(e_1a)^2\nabla^2\right]\left[1-(e_0a)^2\nabla^2\right]\sigma_{ij} = C_{ijkl}\left[1-(e_1a)^2\nabla^2\right]\varepsilon_{kl} - C_{ijkl}\,l^2\left[1-(e_0a)^2\nabla^2\right]\nabla^2\varepsilon_{kl} \tag{33}$$

in which ∇^2 denotes the Laplacian operator. Supposing $e_1 = e_0 = e$ and discarding terms of order $O(\nabla^2)$, the general constitutive relation in Eq. (33) can be rewritten as [42]:

$$[1-(ea)^2\nabla^2]\,\sigma_{ij} = C_{ijkl}\,[1-l^2\nabla^2]\varepsilon_{kl} \tag{34}$$

Thus, the constitutive relations for a nonlocal refined shear deformable FG nanobeam can be stated as:

$$\sigma_{xx} - \mu^2\frac{\partial^2\sigma_{xx}}{\partial x^2} = E(z)\left(\varepsilon_{xx} - \lambda^2\frac{\partial^2\varepsilon_{xx}}{\partial x^2}\right) \tag{35}$$

$$\sigma_{xz} - \mu^2\frac{\partial^2\sigma_{xz}}{\partial x^2} = G(z)\left(\gamma_{xz} - \lambda^2\frac{\partial^2\gamma_{xz}}{\partial x^2}\right) \tag{36}$$

where $\mu = ea$ and $\lambda = l$. By integrating Eqs. (35) and (36) over the cross-sectional area of nanobeam provides the following nonlocal relations for FGM beam model as:

$$N - \mu^2\frac{\partial^2 N}{\partial x^2} = \left(1-\lambda^2\frac{\partial^2}{\partial x^2}\right)\times\left(A\frac{\partial u}{\partial x} - B\frac{\partial^2 w_b}{\partial x^2} - B_s\frac{\partial^2 w_s}{\partial x^2} + Xw_z\right) \tag{37}$$

$$M_b - \mu^2\frac{\partial^2 M_b}{\partial x^2} = \left(1-\lambda^2\frac{\partial^2}{\partial x^2}\right)\times\left(B\frac{\partial u}{\partial x} - D\frac{\partial^2 w_b}{\partial x^2} - D_s\frac{\partial^2 w_s}{\partial x^2} + Yw_z\right) \tag{38}$$

$$M_s - \mu^2\frac{\partial^2 M_s}{\partial x^2} = \left(1-\lambda^2\frac{\partial^2}{\partial x^2}\right)\times\left(B_s\frac{\partial u}{\partial x} - D_s\frac{\partial^2 w_b}{\partial x^2} - H_s\frac{\partial^2 w_s}{\partial x^2} + Y_sw_z\right) \tag{39}$$

$$Q - \mu^2\frac{\partial^2 Q}{\partial x^2} = \left(1-\lambda^2\frac{\partial^2}{\partial x^2}\right)\left(A_s\left(\frac{\partial w_s}{\partial x} + \frac{\partial w_z}{\partial x}\right)\right) \tag{40}$$

$$R_z - \mu^2\frac{\partial^2 R_z}{\partial x^2} = \left(1-\lambda^2\frac{\partial^2}{\partial x^2}\right)\times\left(X\frac{\partial u}{\partial x} - Y\frac{\partial^2 w_b}{\partial x^2} - Y_s\frac{\partial^2 w_s}{\partial x^2} + Zw_z\right) \tag{41}$$

where the cross-sectional rigidities are expressed as:

$$(A,B,B_s,D,D_s,H_s) = \int_{-h/2}^{h/2}\frac{E(z)}{1-v^2(z)}\,(1\,,z,f,z^2,zf,f^2)dz \tag{42}$$

$$A_s = \int_{-h/2}^{h/2} g^2G(z)dz \tag{43}$$

$$(X,Y,Y_s,Z) = \int_{-h/2}^{h/2}\frac{E(z)v(z)}{1-v^2(z)}\,(1\,,z,f,g')g'dz \tag{44}$$

The governing equations of a quasi-3D FG nanobeam in terms of displacements are obtained by inserting for N, M_b, M_s, Q and R_z from Eqs. (37)–(41), respectively, into Eqs. (27)–(30) as follows:

$$A\left(1-\lambda^2\frac{\partial^2}{\partial x^2}\right)\left(\frac{\partial^2 u}{\partial x^2}\right) - B\left(1-\lambda^2\frac{\partial^2}{\partial x^2}\right)\left(\frac{\partial^3 w_b}{\partial x^3}\right) - B_s\left(1-\lambda^2\frac{\partial^2}{\partial x^2}\right)\left(\frac{\partial^3 w_s}{\partial x^3}\right) + X\left(1-\lambda^2\frac{\partial^2}{\partial x^2}\right)\frac{\partial w_z}{\partial x} - I_0\frac{\partial^2 u}{\partial t^2} + I_1\frac{\partial^3 w_b}{\partial x\partial t^2} + J_1\frac{\partial^3 w_s}{\partial x\partial t^2} + \mu^2\left(I_0\frac{\partial^4 u}{\partial x^2\partial t^2} - I_1\frac{\partial^5 w_b}{\partial x^3\partial t^2} - J_1\frac{\partial^5 w_s}{\partial x^3\partial t^2}\right) = 0 \tag{45}$$

$$B\left(1-\lambda^2\frac{\partial^2}{\partial x^2}\right)\left(\frac{\partial^3 u}{\partial x^3}\right)-D\left(1-\lambda^2\frac{\partial^2}{\partial x^2}\right)\left(\frac{\partial^4 w_b}{\partial x^4}\right)$$
$$-D_s\left(1-\lambda^2\frac{\partial^2}{\partial x^2}\right)\left(\frac{\partial^4 w_s}{\partial x^4}\right)$$
$$+Y\left(1-\lambda^2\frac{\partial^2}{\partial x^2}\right)\frac{\partial^2 w_z}{\partial x^2}-\left(N_1^T\right)\frac{\partial^2(w_b+w_s)}{\partial x^2}-\left(N_2^T\right)\frac{\partial^2 w_z}{\partial x^2}$$
$$-I_0\left(\frac{\partial^2 w_b}{\partial t^2}+\frac{\partial^2 w_s}{\partial t^2}\right)-I_1\frac{\partial^3 u}{\partial x\partial t^2}+I_2\frac{\partial^4 w_b}{\partial x^2\partial t^2}+J_2\frac{\partial^4 w_s}{\partial x^2\partial t^2}$$
$$-I_g\frac{\partial^2 w_z}{\partial t^2}+\mu^2\left(\left(N_1^T\right)\frac{\partial^4(w_b+w_s)}{\partial x^4}+\left(N_2^T\right)\frac{\partial^4 w_z}{\partial x^4}\right.$$
$$+I_0\left(\frac{\partial^4 w_b}{\partial x^2\partial t^2}+\frac{\partial^4 w_s}{\partial x^2\partial t^2}\right)+I_1\frac{\partial^5 u}{\partial x^3\partial t^2}-I_2\frac{\partial^6 w_b}{\partial x^4\partial t^2}$$
$$\left.-J_2\frac{\partial^6 w_s}{\partial x^4\partial t^2}+I_g\frac{\partial^2 w_z}{\partial x^2\partial t^2}\right)=0 \tag{46}$$

$$B_s\left(1-\lambda^2\frac{\partial^2}{\partial x^2}\right)\left(\frac{\partial^3 u}{\partial x^3}\right)-D_s\left(1-\lambda^2\frac{\partial^2}{\partial x^2}\right)\left(\frac{\partial^4 w_b}{\partial x^4}\right)$$
$$-H_s\left(1-\lambda^2\frac{\partial^2}{\partial x^2}\right)\left(\frac{\partial^4 w_s}{\partial x^4}\right)+A_s\left(1-\lambda^2\frac{\partial^2}{\partial x^2}\right)$$
$$\times\left(\frac{\partial^2 w_s}{\partial x^2}+\frac{\partial^2 w_z}{\partial x^2}\right)+Y_s\left(1-\lambda^2\frac{\partial^2}{\partial x^2}\right)\left(\frac{\partial^2 w_z}{\partial x^2}\right)$$
$$-\left(N_1^T\right)\frac{\partial^2(w_b+w_s)}{\partial x^2}-\left(N_2^T\right)\frac{\partial^2 w_z}{\partial x^2}-I_0\left(\frac{\partial^2 w_b}{\partial t^2}+\frac{\partial^2 w_s}{\partial t^2}\right)$$
$$-J_1\frac{\partial^3 u}{\partial x\partial t^2}+J_2\frac{\partial^4 w_b}{\partial x^2\partial t^2}+K_2\frac{\partial^4 w_s}{\partial x^2\partial t^2}-I_g\frac{\partial^2 w_z}{\partial t^2}$$
$$+\mu^2\left(\left(N_1^T\right)\frac{\partial^4(w_b+w_s)}{\partial x^4}+\left(N_2^T\right)\frac{\partial^4 w_z}{\partial x^4}\right.$$
$$+I_0\left(\frac{\partial^4 w_b}{\partial x^2\partial t^2}+\frac{\partial^4 w_s}{\partial x^2\partial t^2}\right)+J_1\frac{\partial^5 u}{\partial x^3\partial t^2}-J_2\frac{\partial^6 w_b}{\partial x^4\partial t^2}$$
$$\left.-K_2\frac{\partial^6 w_s}{\partial x^4\partial t^2}+I_g\frac{\partial^2 w_z}{\partial x^2\partial t^2}\right)=0 \tag{47}$$

$$-X\left(1-\lambda^2\frac{\partial^2}{\partial x^2}\right)\left(\frac{\partial u}{\partial x}\right)+Y\left(1-\lambda^2\frac{\partial^2}{\partial x^2}\right)\left(\frac{\partial^2 w_b}{\partial x^2}\right)$$
$$+(A_s+Y_s)\left(1-\lambda^2\frac{\partial^2}{\partial x^2}\right)\left(\frac{\partial^2 w_s}{\partial x^2}\right)$$
$$+A_s\left(1-\lambda^2\frac{\partial^2}{\partial x^2}\right)\frac{\partial^2 w_z}{\partial x^2}-Z\left(1-\lambda^2\frac{\partial^2}{\partial x^2}\right)w_z$$
$$-\left(N_1^T\right)\frac{\partial^2(w_b+w_s)}{\partial x^2}-\left(N_2^T\right)\frac{\partial^2 w_z}{\partial x^2}$$
$$-I_g\left(\frac{\partial^2 w_b}{\partial t^2}+\frac{\partial^2 w_s}{\partial t^2}\right)-K_g\left(\frac{\partial^2 w_z}{\partial t^2}\right)$$
$$+\mu^2\left(\left(N_1^T\right)\frac{\partial^4(w_b+w_s)}{\partial x^4}+\left(N_2^T\right)\frac{\partial^4 w_z}{\partial x^4}\right.$$
$$\left.+I_g\left(\frac{\partial^4 w_b}{\partial x^2\partial t^2}+\frac{\partial^4 w_s}{\partial x^2\partial t^2}\right)+K_g\left(\frac{\partial^2 w_z}{\partial x^2\partial t^2}\right)\right)=0. \tag{48}$$

3 Solution procedure

The solution of governing equations of nonlocal FGM nanobeam can be presented by:

$$u(x,t)=U_n\exp[i(\beta x-\omega t)] \tag{49}$$
$$w_b(x,t)=W_{bn}\exp[i(\beta x-\omega t)] \tag{50}$$
$$w_s(x,t)=W_{sn}\exp[i(\beta x-\omega t)] \tag{51}$$
$$w_z(x,t)=W_{zn}\exp[i(\beta x-\omega t)] \tag{52}$$

In which $(U_n, W_{bn}, W_{sn}, W_{zn})$ are the wave amplitudes; β and ω denote the wave number and circular frequency, respectively. Inserting Eqs. (49)–(52) into Eqs. (45)–(48) gives:

$$\left\{[K]_{4\times4}-\omega^2[M]_{4\times4}\right\}\begin{Bmatrix}U_n\\W_{bn}\\W_{sn}\\W_{zn}\end{Bmatrix}=0 \tag{53}$$

where

$$k_{1,1} = -A\beta^2 - \lambda^2 A\beta^4, \quad k_{1,2} = -iB\beta^3 - i\lambda^2 B\beta^5, \quad k_{2,1} = +iB\beta^3 + i\lambda^2 B\beta^3,$$
$$k_{1,3} = -iB_s\beta^3 - i\lambda^2 B_s\beta^5, \quad k_{1,4} = -Xi\beta - X\lambda^2 i\beta^3, \quad k_{4,1} = +Xi\beta + X\lambda^2 i\beta^3,$$
$$k_{2,4} = -Y\beta^2 - \lambda^2 Y\beta^4 + N_1^T\beta^2(1+\mu^2\beta^2), \quad k_{4,2} = -Y\beta^2 - \lambda^2 Y\beta^4 + N_2^T\beta^2(1+\mu^2\beta^2),$$
$$k_{3,1} = +iB_s\beta^3 + i\eta B\beta^5, \quad k_{2,3} = N_1^T\beta^2(1+\mu^2\beta^2) - D_s\beta^4 - \lambda^2 D_s\beta^6,$$
$$k_{2,2} = N_1^T\beta^2(1+\mu^2\beta^2) - D\beta^4 - \lambda^2 D\beta^6, \quad k_{3,3} = N_1^T\beta^2(1+\mu^2\beta^2) - A_s\beta^2 - H_s\beta^4 - \lambda^2 H_s\beta^6 - \lambda^2 A\beta^4,$$
$$k_{3,4} = -(A_s + Y_s)\beta^2 - \lambda^2(A_s + Y_s)\beta^4 + N_1^T\beta^2(1+\mu^2\beta^2), \quad k_{4,4} = -A_s\beta^2 - \lambda^2 A_s\beta^4 - Z - \lambda^2 Z\beta^2 + N_2^T\beta^2(1+\mu^2\beta^2)$$
$$m_{1,1} = I_0(1+\mu\beta^2), \quad m_{1,2} = +iI_1\beta + i\mu^2 I_1\beta^3, \quad m_{2,1} = -iI_1\beta - i\mu^2 I_1\beta^3$$
$$m_{1,3} = +iJ_1\beta + i\mu^2 J_1\beta^3, \quad m_{3,1} = -iJ_1\beta - i\mu^2 J_1\beta^3, \quad m_{1,4} = 0, \quad m_{2,4} = m_{3,4} = I_g(1+\mu^2\beta^2),$$
$$m_{2,2} = I_0(1+\mu^2\beta^2) + I_2\beta^2 + \mu^2 I_2\beta^4, \quad m_{4,2} = m_{4,3} = I_g(1+\mu^2\beta^2),$$
$$m_{2,3} = I_0(1+\mu^2\beta^2) + J_2\beta^2 + \mu^2 J_2\beta^4, \quad m_{3,3} = I_0(1+\mu^2\beta^2) + K_2\beta^2 + \mu^2 K_2\beta^4,$$
$$m_{4,4} = K_g(1+\mu^2\beta^2),$$

By setting the determinant of above matrix to zero, the circular frequency ω can be obtained. Hence, the roots of Eq. (45) can be expressed by:

$$\omega_1 = M_0(\beta), \quad \omega_2 = M_1(\beta), \quad \omega_3 = M_2(\beta) \tag{54}$$

These roots are corresponded with the wave modes M_0, M_1 and M_2, respectively. The wave modes M_0, M_2 are related to the flexural waves, and mode M_1 is related to the extensional waves. Also, the phase velocity of waves can be calculated by the following relation:

$$c_{p\,(i)} = \frac{M_i(\beta)}{\beta}, \quad i = 1, 2, 3 \tag{55}$$

which displays the dispersion relation of phase velocity c_p and wave number β for the FGM nanobeam. Also, the escape frequencies of FGM nanobeam can be calculated by setting $\beta \to \infty$. It is worth mentioning that after the escape frequency, the flexural waves will not propagate anymore. And the group velocity of wave propagation in a FG plate can be expressed as:

$$c_{g(i)} = \frac{\partial M_i(\beta)}{\partial \beta} \quad (i = 1, 2, 3). \tag{56}$$

4 Numerical results and discussions

A nonlocal strain gradient theory is developed for wave dispersion analysis of quasi-3D FG nanobeams in thermal environments. The thickness of nanobeam shown in Fig. 1 is considered as $h = 100$ nm. In Table 2, comparison of frequencies of FG nanobeams with those of presented by Ebrahimi and Salari [25] is presented. In this table, frequency results are presented for various gradient indices and nonlocality parameters at $L/h = 20$, while thickness stretching is neglected ($\varepsilon_z = 0$). The results of present study are in good agreement with the previous ones.

Variation of the wave frequency ($f = \omega/2\pi$) of FG nanobeam versus wave number (β) for different temperature changes ($\Delta T = 0$, 200, 500, 800 K) at a fixed gradient index ($p = 1$) and nonlocal parameter $\mu = 1$ nm according to various wave modes is illustrated in Fig. 2. It is observed that for $\beta \leq 0.1$, temperature changes have no observable effect on the wave frequency, but for higher values of wave number, the temperature effect is more considerable. With the increase in temperature, wave frequencies reduce especially at higher values of wave number. So, effect of temperature change on wave frequency depends on the value of wave number. Also, increasing wave number lead to higher frequencies according to nonlocal strain gradient theory ($\lambda = 1$ nm). Moreover, when $l = 0$, wave number has no sensible effect on wave frequencies.

Influence of temperature rise (ΔT) and length scale parameter (λ) on the phase velocity (c_p) of FG nanobeam versus wave number at $p = 1$ and $\mu = 1$ nm is depicted in Fig. 3. It is found that for $\beta \leq 0.1$, changing length scale

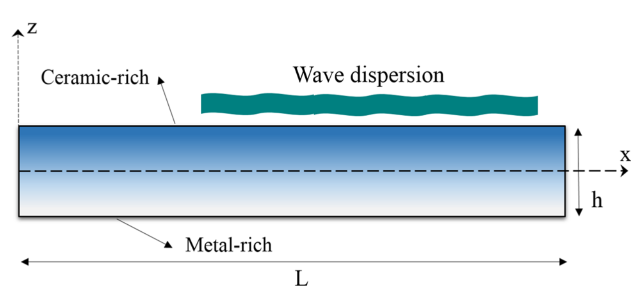

Fig. 1 Geometry and coordinates of functionally graded nanobeam. **a** M_0 mode, **b** M_1 mode and **c** M_2 mode

Table 2 Comparison of the frequency of a Mori–Tanaka based FG nanobeam without elastic foundation ($L/h = 20$)

μ	Gradient index (p)							
	0		0.2		1		5	
	EBT [25]	Present	EBT [25]	Present	EBT [25]	Present	EBT [25]	Present
0	9.8594	9.82961	8.5788	8.55415	6.9131	6.89568	5.8869	5.86719
1	9.4062	9.37773	8.1844	8.16086	6.5953	6.57866	5.6163	5.59746
2	9.0102	8.98293	7.8399	7.81730	6.3176	6.30170	5.3798	5.36182
3	8.6603	8.63414	7.5354	7.51376	6.0723	6.05701	5.1709	5.15362
4	8.3483	8.32306	7.2639	7.24305	5.8536	5.83878	4.9846	4.96794

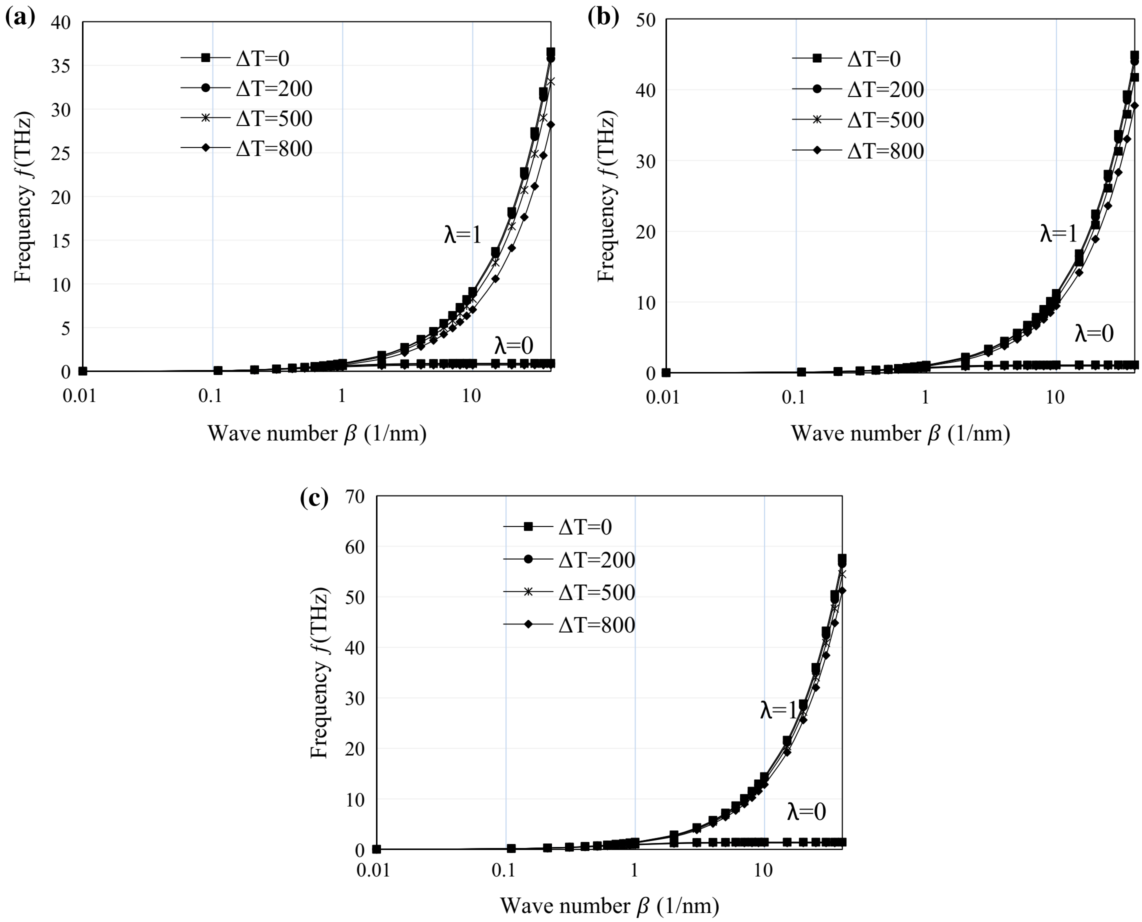

Fig. 2 Influence of temperature rise and length scale parameter on the frequency of temperature-dependent FG nanobeam for various wave modes ($\mu = 1$ nm, $p = 1$). **a** M_0 mode, **b** M_1 mode and **c** M_2 mode

parameter has no effect on the phase velocity, but the effect of length scale parameter on phase velocity becomes prominent at higher values of wave number in a constant temperature change. Also, it is observable that phase velocity tends to be constant with the change in wave number for higher value of wave number. Also, irrespective of the value of length scale parameter, increasing temperature leads to reduction in phase velocities. When length scale parameter is zero ($\lambda = 0$), effect of temperature change becomes less important at higher wave modes.

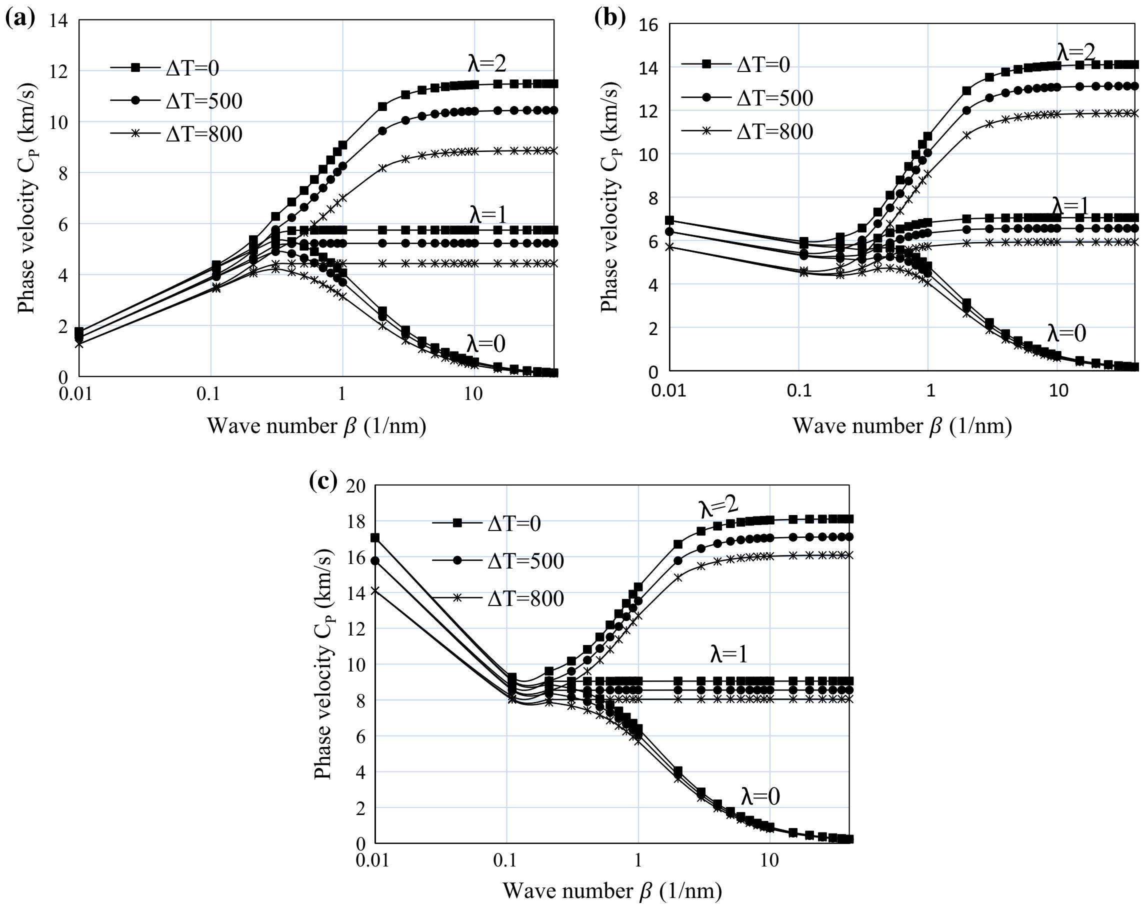

Fig. 3 Influence of temperature rise and length scale parameter on the phase velocity of temperature-dependent FG nanobeam for various wave modes ($\mu = 1$ nm, $p = 1$). **a** M_0 mode, **b** M_1 mode and **c** M_2 mode

Variation of phase velocity of FG nanobeams versus wave number is demonstrated in Fig. 4 for various gradient indices and length scale parameters when $\mu = 1$ nm and $\Delta T = 800$. It is found that for $\beta \leq 0.1$, the effect of length scale parameter on phase velocity can be neglected in constant gradient index. Also, it is deduced that for larger values of wave number, the phase velocity becomes constant and does not change with the increase in wave number for every value of gradient index. Also, it is found that increasing gradient index leads to lower phase velocities at a fixed nonlocal and length scale parameters.

Influence of nonlocality parameter on the phase velocity of FG nanobeam is plotted with respect to wave number when $p = 1$ and $\Delta T = 800$. One can see that influence of nonlocal parameter on phase velocities depends on the value of wave number. In fact, effect of nonlocal parameter is remarkable only for larger wave numbers. However, increasing nonlocal parameter decreases the phase velocity regardless of the value of length scale parameter. Also, at $\lambda = 0$ by increasing wave number, the phase velocity approaches to zero, and effect of nonlocal parameter becomes less sensible (Fig. 5).

Group velocity (c_g) as a function of temperature rise, length scale parameter and wave number when $p = 1$ is shown in Fig. 6. It can be deduced that for lower wave numbers, the group velocity of different length scale parameters are not detectable from each other. But, the group velocities become distinguished at higher values of wave number. It is clear that at a fixed length scale

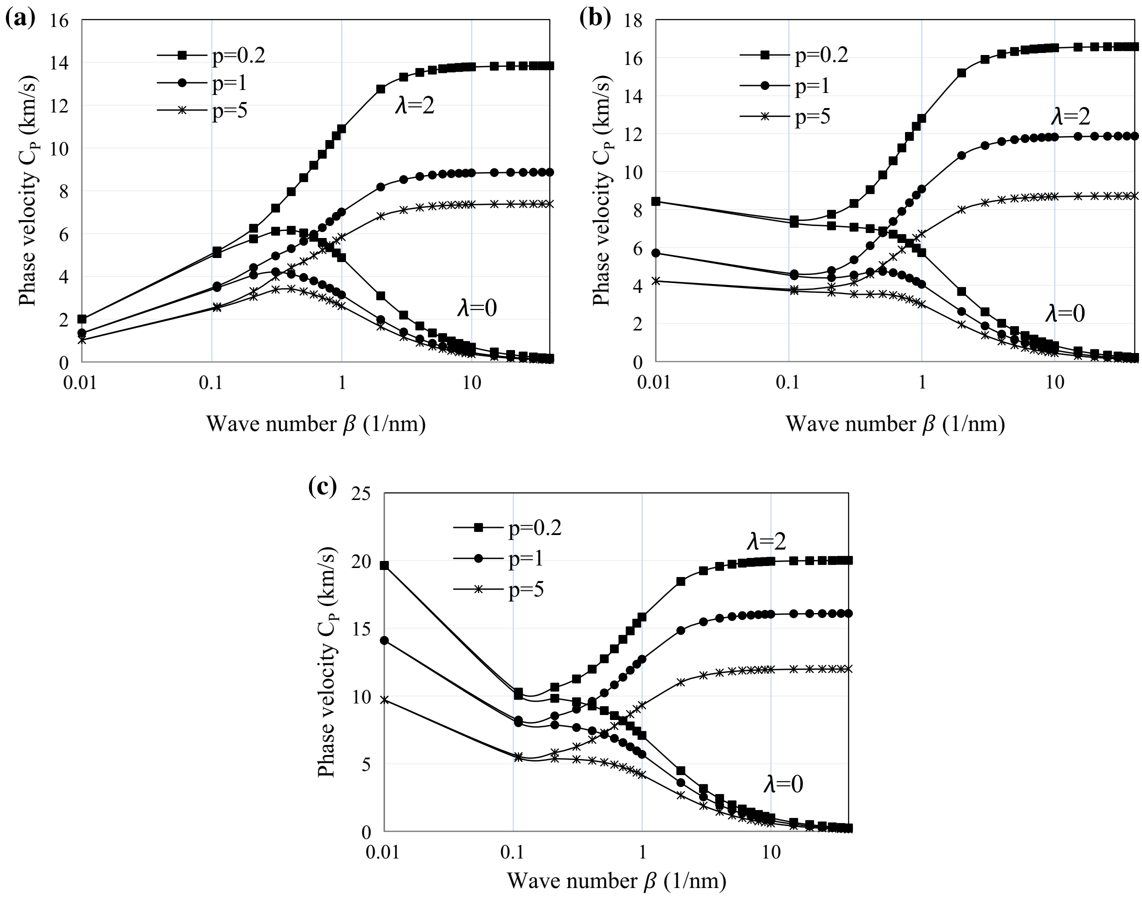

Fig. 4 The effect of diverse gradient index and Length scale parameter on the phase velocity of temperature-dependent FG nanobeam for various wave modes ($\mu = 1$, $\Delta T = 800$). **a** M_0 mode, **b** M_1 mode and **c** M_2 mode

parameter, the group velocity decreases by increasing in temperature. Also, at $\lambda = 0$ and higher wave numbers, effect of temperature change on group velocities is not notable. Furthermore, due to stiffness-hardening effect of length scale parameter introduced by nonlocal strain gradient theory, the group velocities are increased with the rise of length scale parameter.

Figure 7 indicates the impact of gradient index on the group velocity of temperature-dependent FG nanobeam with respect to wave number (β) at $\Delta T = 800$ and $\mu = 1$ nm. It is concluded that at a constant wave number and length scale parameter, with the increase in gradient index, the group velocity decreases. In fact, higher values of gradient index are correspond to lower portion of ceramic phase in FG nanobeams. Thus, increasing gradient index shows a reducing effect on the wave characteristics of FG nanobeams. This is due to higher portion of metal phase with increase in gradient index.

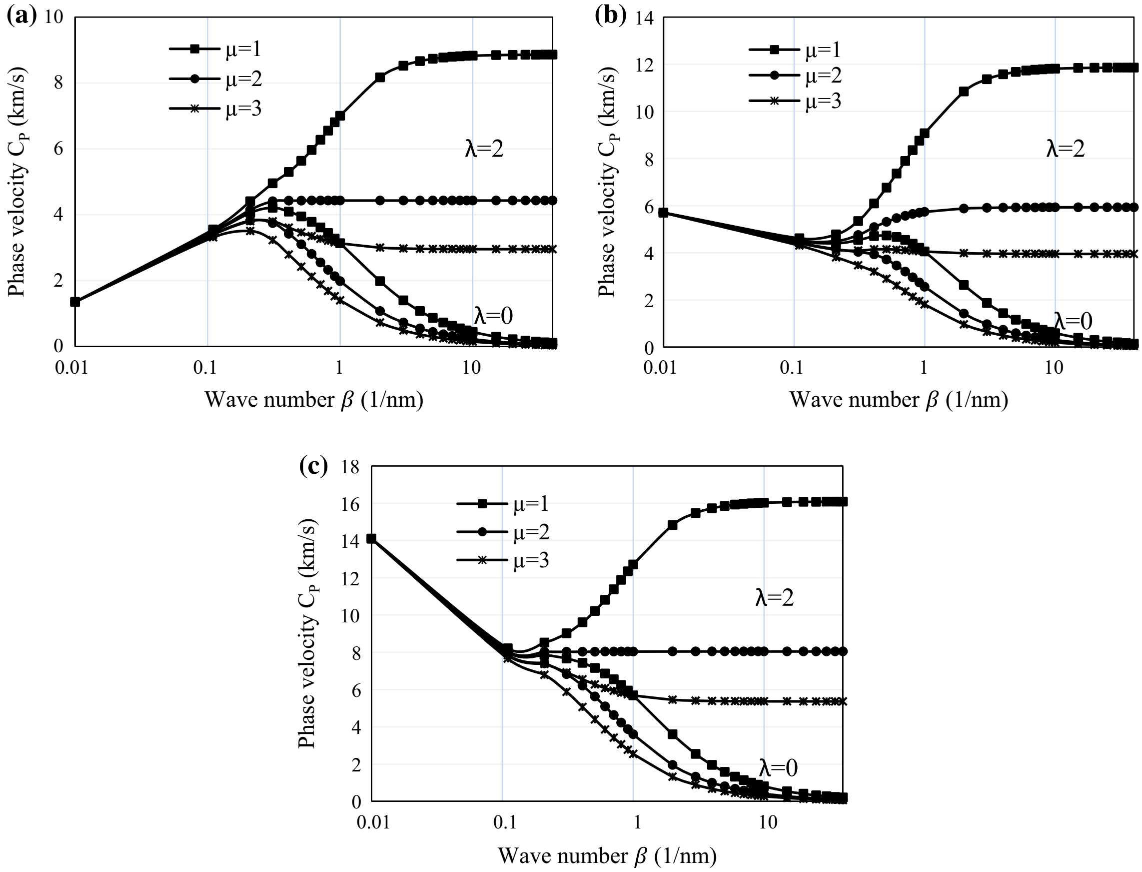

Fig. 5 The effect of various nonlocality parameter and length scale parameter on the temperature-dependent FG nanobeam for various wave modes ($\Delta T = 800$, $p = 1$). **a** M_0 mode, **b** M_1 mode and **c** M_2 mode

Figure 8 illustrates the variation of escape frequencies of nonlocal strain gradient FG nanobeams with changing of gradient index when $\mu = \lambda = 1$ nm. To this purpose, the wave number is set to infinity. It is clear that with the increase in gradient index the escape frequency decreases, especially at lower gradient indices. Furthermore, it is observable that the escape frequencies of different temperatures are more distinguished at higher values of gradient index. Also, it is observable that with the increase in temperature in constant gradient index escape frequency reduces.

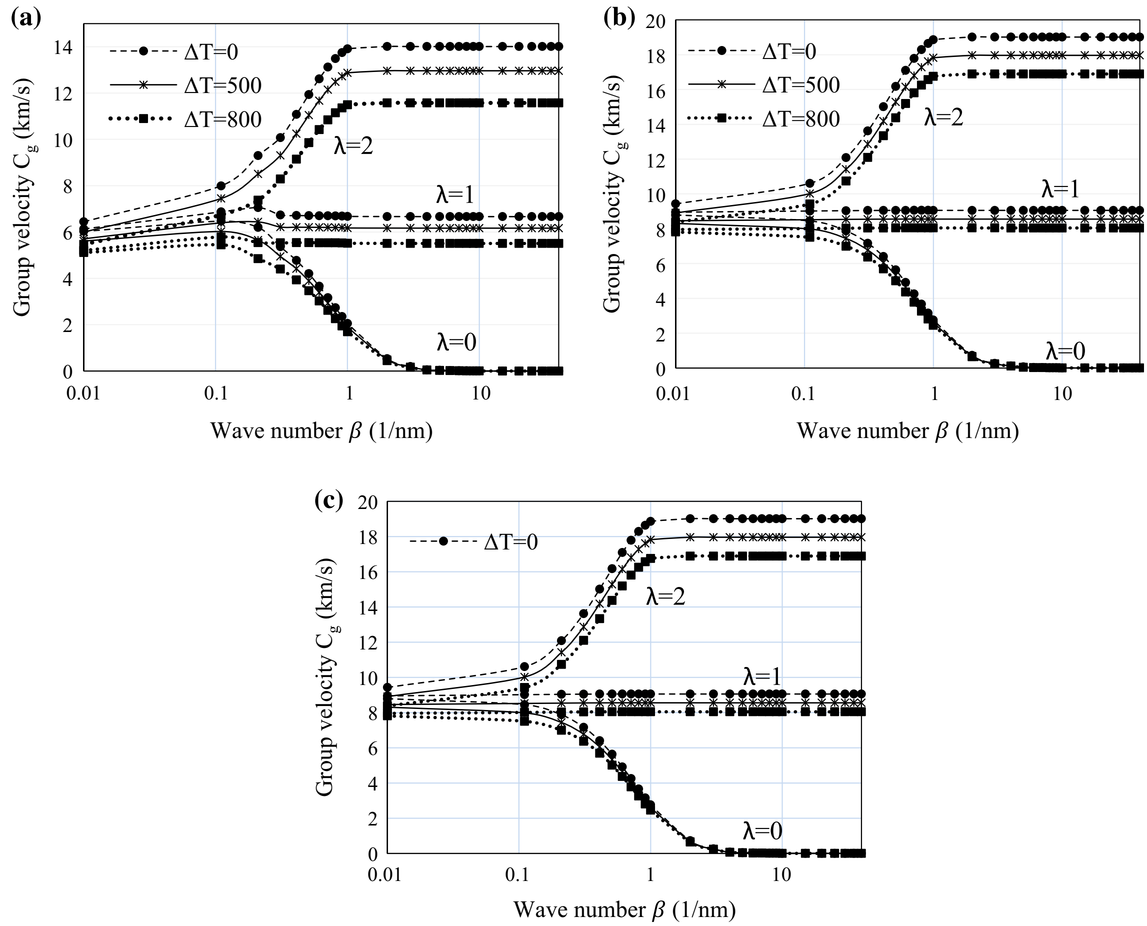

Fig. 6 Effect of different temperatures and length scale parameters on the group velocity of temperature-dependent FG nanobeam for various wave modes ($p = 1$). **a** M_0 mode, **b** M_1 mode and **c** M_2 mode

5 Conclusions

In this article, nonlocal strain gradient theory which contains both nonlocal and length scale parameters for more accurate description of size effects is employed to examine the wave propagation behavior of size-dependent FG nanobeams in thermal environments. The material properties of nanobeam change gradually through the thickness via Mori–Tanaka scheme and are considered to be temperature-dependent. The governing equations of FG

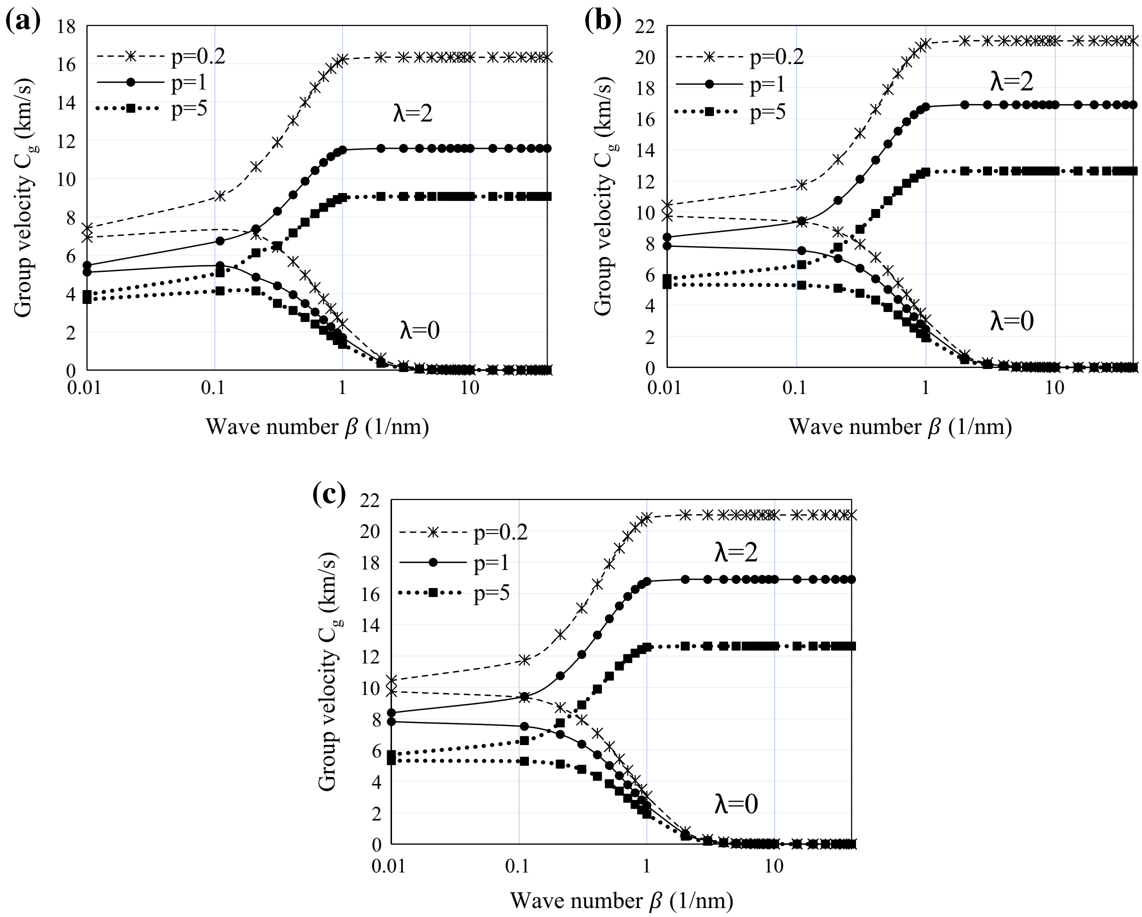

Fig. 7 The effect of various gradient index and length scale parameter on the group velocity of temperature-dependent FG nanobeam ($\Delta T = 800$, $\mu = 1$). **a** M_0 mode, **b** M_1 mode and **c** M_2 mode

nanobeam modeled via a quasi-3D sinusoidal theory are derived by using Hamilton's principle. An analytical solution is applied to find the wave frequency, escape frequency and phase velocities of FG nanoplate. It is observed that the wave frequency, phase velocity, group velocity and escape frequency decrease with the increase in temperature. Also, nonlocal parameter has a stiffness-softening influence and reduces the phase velocities. Also, length scale parameter possesses a stiffness-hardening effect and increases the phase velocities and escape frequencies. The gradient index has a considerable decreasing influence on the phase velocities and escape frequencies.

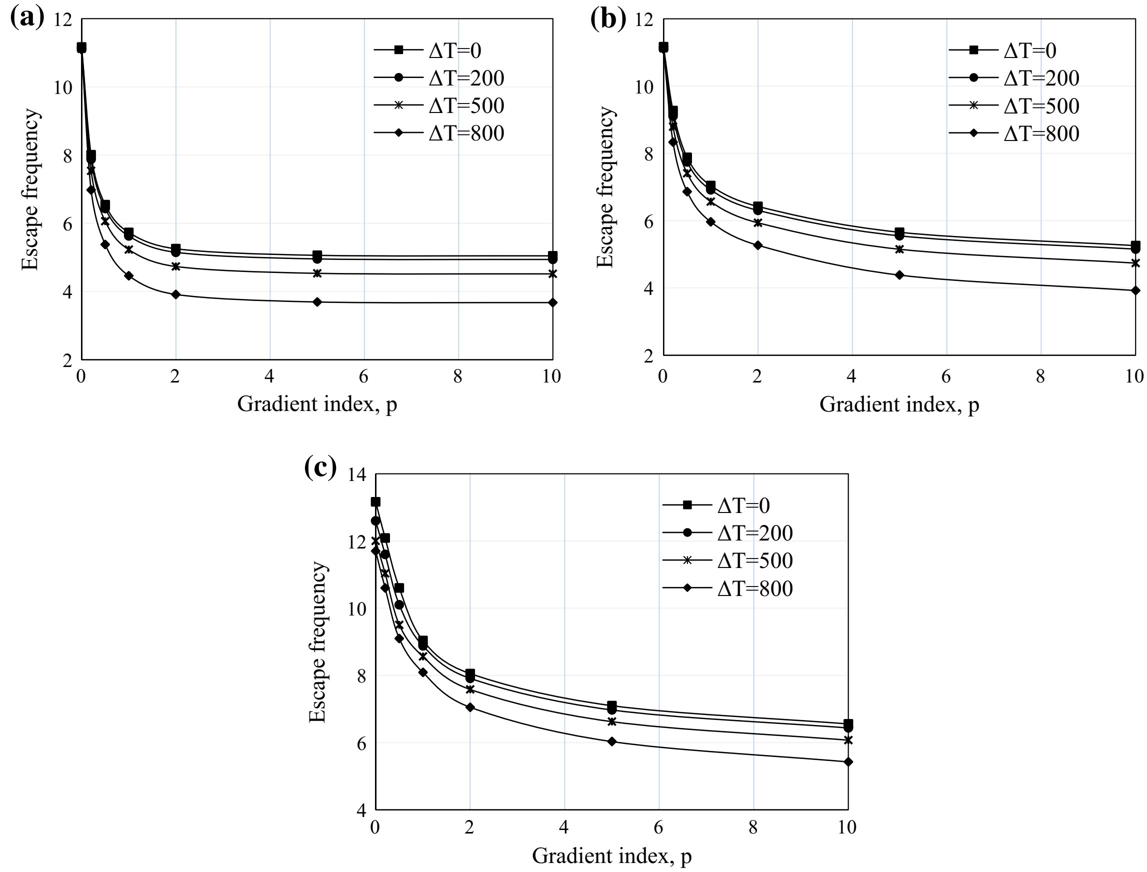

Fig. 8 Effect of gradient index and nonlinear temperature changes on the escape frequency of FG nanobeam for various wave modes ($\mu = 1$ nm^2, $l = 1$ nm^2). **a** M_0 mode, **b** M_1 mode and **c** M_2 mode

Also, when the effect of length scale parameter is omitted, the nonlocal parameter and gradient index have no important influence on phase velocity at larger wave numbers.

References

1. A. Tounsi, M.S.A. Houari, S. Benyoucef, A refined trigonometric shear deformation theory for thermoelastic bending of functionally graded sandwich plates. Aerosp. Sci. Technol. **24**(1), 209–220 (2013)
2. M. Zidi, A. Tounsi, M.S.A. Houari, O.A. Bég, Bending analysis of FGM plates under hygro-thermo-mechanical loading using a four variable refined plate theory. Aerosp. Sci. Technol. **34**, 24–34 (2014)
3. A. Hamidi, M.S.A. Houari, S.R. Mahmoud, A. Tounsi, A sinusoidal plate theory with 5-unknowns and stretching effect for thermomechanical bending of functionally graded sandwich plates. Steel Compos. Struct. **18**(1), 235–253 (2015)
4. A. Tounsi, S. Benguediab, B. Adda, A. Semmah, M. Zidour, Nonlocal effects on thermal buckling properties of double-walled carbon nanotubes. Adv. Nano Res. **1**(1), 1–11 (2013)
5. A. Chakraborty, S. Gopalakrishnan, A spectral finite element for axial–flexural–shear coupled wave propagation analysis in lengthwise graded beam. Comput. Mech. **36**(1), 1–12 (2005)
6. A. Chakraborty, S. Gopalakrishnan, A spectrally formulated finite element for wave propagation analysis in functionally graded beams. Int. J. Solids Struct. **40**(10), 2421–2448 (2003)
7. D. Sun, S.N. Luo, Wave propagation and transient response of a FGM plate under a point impact load based on higher-order shear deformation theory. Compos. Struct. **93**(5), 1474–1484 (2011)
8. D. Sun, S.N. Luo, Wave propagation of functionally graded material plates in thermal environments. Ultrasonics **51**(8), 940–952 (2011)
9. W.Q. Chen, H.M. Wang, R.H. Bao, On calculating dispersion curves of waves in a functionally graded elastic plate. Compos. Struct. **81**(2), 233–242 (2007)
10. S.A. Yahia, H.A. Atmane, M.S.A. Houari, A. Tounsi, Wave propagation in functionally graded plates with porosities using various higher-order shear deformation plate theories. Struct. Eng. Mech. **53**(6), 1143 (2015)
11. M.A.A. Meziane, H.H. Abdelaziz, A. Tounsi, An efficient and simple refined theory for buckling and free vibration of exponentially graded sandwich plates under various boundary conditions. J. Sandwich Struct. Mater. **16**(3), 293–318 (2014)
12. H. Bellifa, K.H. Benrahou, L. Hadji, M.S.A. Houari, A. Tounsi, Bending and free vibration analysis of functionally graded plates using a simple shear deformation theory and the concept the

neutral surface position. J. Braz. Soc. Mech. Sci. Eng. **38**, 265–275 (2016)
13. K.S. Al-Basyouni, A. Tounsi, S.R. Mahmoud, Size dependent bending and vibration analysis of functionally graded micro beams based on modified couple stress theory and neutral surface position. Compos. Struct. **125**, 621–630 (2015)
14. S. Benguediab, A. Tounsi, M. Zidour, A. Semmah, Chirality and scale effects on mechanical buckling properties of zigzag double-walled carbon nanotubes. Compos. B Eng. **57**, 21–24 (2014)
15. A.C. Eringen, D.G.B. Edelen, On nonlocal elasticity. Int. J. Eng. Sci. **10**(3), 233–248 (1972)
16. A.C. Eringen, On differential equations of nonlocal elasticity and solutions of screw dislocation and surface waves. J. Appl. Phys. **54**(9), 4703–4710 (1983)
17. Y. Yang, L. Zhang, C.W. Lim, Wave propagation in double-walled carbon nanotubes on a novel analytically nonlocal Timoshenko-beam model. J. Sound Vib. **330**(8), 1704–1717 (2011)
18. A. Assadi, B. Farshi, Size-dependent longitudinal and transverse wave propagation in embedded nanotubes with consideration of surface effects. Acta Mech. **222**(1–2), 27–39 (2011)
19. S. Narendar, S.S. Gupta, S. Gopalakrishnan, Wave propagation in single-walled carbon nanotube under longitudinal magnetic field using nonlocal Euler–Bernoulli beam theory. Appl. Math. Model. **36**(9), 4529–4538 (2012)
20. A.G. Arani, R. Kolahchi, S.A. Mortazavi, Nonlocal piezoelasticity based wave propagation of bonded double-piezoelectric nanobeam-systems. Int. J. Mech. Mater. Des. **10**(2), 179–191 (2014)
21. M.A. Eltaher, M.E. Khater, S.A. Emam, A review on nonlocal elastic models for bending, buckling, vibrations, and wave propagation of nanoscale beams. Appl. Math. Model. **40**(5), 4109–4128 (2016)
22. C.F. Lü, C.W. Lim, W.Q. Chen, Size-dependent elastic behavior of FGM ultra-thin films based on generalized refined theory. Int. J. Solids Struct. **46**(5), 1176–1185 (2009)
23. M. Rahaeifard, M.H. Kahrobaiyan, M.T. Ahmadian, Sensitivity analysis of atomic force microscope cantilever made of functionally graded materials, in *ASME 2009 International Design Engineering Technical Conferences and Computers and Information in Engineering Conference* (American Society of Mechanical Engineers, New York, 2009), pp. 539–544
24. M.A. Eltaher, S.A. Emam, F.F. Mahmoud, Free vibration analysis of functionally graded size-dependent nanobeams. Appl. Math. Comput. **218**(14), 7406–7420 (2012)
25. F. Ebrahimi, E. Salari, Thermo-mechanical vibration analysis of nonlocal temperature-dependent FG nanobeams with various boundary conditions. Compos. B Eng. **78**, 272–290 (2015)
26. F. Ebrahimi, M.R. Barati, Dynamic modeling of a thermo–piezo-electrically actuated nanosize beam subjected to a magnetic field. Appl. Phys. A **122**(4), 1–18 (2016)
27. F. Ebrahimi, M.R. Barati, Vibration analysis of smart piezoelectrically actuated nanobeams subjected to magneto-electrical field in thermal environment. J. Vib. Control (2016). doi:10.1177/1077546316646239
28. F. Ebrahimi, M.R. Barati, An exact solution for buckling analysis of embedded piezoelectro-magnetically actuated nanoscale beams. Adv. Nano Res. **4**(2), 65–84 (2016)
29. F. Ebrahimi, M.R. Barati, Electromechanical buckling behavior of smart piezoelectrically actuated higher-order size-dependent graded nanoscale beams in thermal environment. Int. J. Smart Nano Mater. **7**(2), 69–90 (2016)
30. F. Ebrahimi, M.R. Barati, Magnetic field effects on buckling behavior of smart size-dependent graded nanoscale beams. Eur. Phys. J. Plus **131**(7), 1–14 (2016)
31. F. Ebrahimi, M.R. Barati, Small scale effects on hygro-thermo-mechanical vibration of temperature dependent nonhomogeneous nanoscale beams. Mech. Adv. Mater. Struct. (2016). doi:10.1080/15376494.2016.1196795
32. A. Tounsi, A. Zemri, M.S.A. Houari, A.A. Bousahla, A mechanical response of functionally graded nanoscale beam: an assessment of a refined nonlocal shear deformation theory beam theory. Struct. Eng. Mech. **54**(4), 693 (2015)
33. F. Bounouara, K.H. Benrahou, I. Belkorissat, A. Tounsi, A nonlocal zeroth-order shear deformation theory for free vibration of functionally graded nanoscale plates resting on elastic foundation. Steel Compos. Struct. **20**(2), 227–249 (2016)
34. I. Belkorissat, M.S.A. Houari, A. Tounsi, E.A. Bedia, S.R. Mahmoud, On vibration properties of functionally graded nano-plate using a new nonlocal refined four variable model. Steel Compos. Struct. **18**(4), 1063–1081 (2015)
35. M.R. Barati, H. Shahverdi, An analytical solution for thermal vibration of compositionally graded nanoplates with arbitrary boundary conditions based on physical neutral surface position. Mech. Adv. Mater. Struct. (2016). doi:10.1080/15376494.2016.1196788
36. M. Bourada, A. Kaci, M.S.A. Houari, A. Tounsi, A new simple shear and normal deformations theory for functionally graded beams. Steel Compos. Struct. **18**(2), 409–423 (2015)
37. H. Hebali, A. Tounsi, M.S.A. Houari, A. Bessaim, E.A.A. Bedia, New quasi-3D hyperbolic shear deformation theory for the static and free vibration analysis of functionally graded plates. J. Eng. Mech. **140**(2), 374–383 (2014)
38. Z. Belabed, M.S.A. Houari, A. Tounsi, S.R. Mahmoud, O.A. Bég, An efficient and simple higher order shear and normal deformation theory for functionally graded material (FGM) plates. Compos. B Eng. **60**, 274–283 (2014)
39. D.C.C. Lam, F. Yang, A.C.M. Chong, J. Wang, P. Tong, Experiments and theory in strain gradient elasticity. J. Mech. Phys. Solids **51**(8), 1477–1508 (2003)
40. C.W. Lim, G. Zhang, J.N. Reddy, A higher-order nonlocal elasticity and strain gradient theory and its applications in wave propagation. J. Mech. Phys. Solids **78**, 298–313 (2015)
41. L. Li, X. Li, Y. Hu, Free vibration analysis of nonlocal strain gradient beams made of functionally graded material. Int. J. Eng. Sci. **102**, 77–92 (2016)
42. L. Li, Y. Hu, L. Ling, Flexural wave propagation in small-scaled functionally graded beams via a nonlocal strain gradient theory. Compos. Struct. **133**, 1079–1092 (2015)
43. F. Ebrahimi, M.R. Barati, Flexural wave propagation analysis of embedded S-FGM nanobeams under longitudinal magnetic field based on nonlocal strain gradient theory. Arab. J. Sci. Eng. (2016). doi:10.1007/s13369-016-2266-4
44. F. Ebrahimi, M.R. Barati, A. Dabbagh, A nonlocal strain gradient theory for wave propagation analysis in temperature-dependent inhomogeneous nanoplates. Int. J. Eng. Sci. **107**, 169–182 (2016)